

Null trajectories and bending of light in charged black holes with quintessence

Sharmanthie Fernando ¹, Scott Meadows ², and Kevon Reis ³

Department of Physics & Geology

Northern Kentucky University

Highland Heights

Kentucky 41099

U.S.A.

Abstract

We have studied null geodesics of the charged black hole surrounded by quintessence. Quintessence is a candidate for dark energy and is represented by a scalar field. Here, we have done a detailed study of the photon trajectories. The exact solutions for the trajectories are obtained in terms of the Jacobi-elliptic integrals for all possible energy and angular momentum of the photons. We have also studied the bending angle using the Rindler and Ishak method.

Key words: static, charged, quintessence, null geodesics, deflection of light

1 Introduction

Recent observations support that the universe is undergoing expansion at an accelerated rate [1][2]. The unknown cause for this cosmic acceleration is known as “dark energy” which consists of about 70% of the energy density of the universe. Understanding the nature of this unknown energy component in the universe is one of the greatest challenges in modern cosmology. An interesting review related to dark energy is given in [3]. A thermodynamic motivation for dark energy can be found in [4]. Observational constraints on dark energy can be found in [5].

The equation of state parameter for dark energy is given by $\omega = \frac{P}{\rho}$. Here P is the pressure and ρ is the energy density of the dark energy. For acceleration to occur, the pressure has to be negative. There are large number of surveys proposed to find the value of ω and its time evolution [6] [7]. .

¹fernando@nku.edu

²meadowss3@mymail.nku.edu

³reisk3@mymail.nku.edu

One of the candidates for dark energy density considered in literature is the cosmological constant with a state parameter $\omega = -1$. There is a major problem that is yet to be understood about the cosmological constant from a fundamental physics point of view. The observed value is too small in comparison with the theoretical prediction and this is well known as the fine-tuning problem [8].

Current observations seems to be consistent with a value of $\omega = -1$. However, these observations say relatively little as to how ω evolve with time. Therefore, it is important to consider alternative models of dark energy where the equation of state changes with time, such as in inflationary cosmology. So far, wide variety of dark energy models with dynamical scalar fields have been proposed as alternative models to cosmological constant. Such scalar field models include, but not limited to, quintessence, K-essence, ghost condensates, phantoms, and dilaton dark energy. A review of the quintessence can be found in [9] [10].

In this paper we focus on quintessence as the candidate for dark energy. Quintessence is described by a scalar field minimally coupled to gravity with the action,

$$S_{quintessence} = \int d^4x \sqrt{-g} (-\partial_\mu \Phi \partial^\mu \Phi - V(\Phi)) \quad (1)$$

The energy momentum tensor for such a field is given by,

$$T_{\mu\nu} = \partial_\mu \Phi \partial_\nu \Phi - g_{\mu\nu} \left(\frac{1}{2} \partial^\sigma \Phi \partial_\sigma \Phi + V(\Phi) \right) \quad (2)$$

For example, in a flat Friedmann-Robertson-Walker universe, the expressions for pressure and energy density for the quintessence is given by,

$$\rho_q = T_0^0 = \frac{\dot{\Phi}^2}{2} + V(\Phi) \quad (3)$$

$$P_q = T_1^1 = \frac{\dot{\Phi}^2}{2} - V(\Phi) \quad (4)$$

For an accelerated universe, $\frac{\dot{\Phi}^2}{2} < V(\Phi)$. Hence for acceleration to occur, the field Φ should vary slowly along the potential $V(\Phi)$. Such a requirement is similar to the slow-roll inflation of the early universe. In addition to the above requirement, for acceleration to occur, the mass of the quintessence $m_\Phi = \sqrt{\frac{d^2V}{d\Phi^2}}$ needs to be very small. This means $m_\Phi \leq H_0 \approx 10^{-33} eV$ where H_0 is the Hubble parameter today.

Many different potentials for the quintessence have been studied in the literature. Depending on how the state parameter evolve in these models, quintessence models are classified in two classes: One is the thawing model. In this case, the field freezes during the cosmological epoch and restart to evolve once the mass of the field drops to a very small value. The second model is the freezing model. Here, the potential tends to be shallow at late times leading the field to slow down. For example, a freezing model can have the potential,

$$V(\Phi) = M^{4+p} \Phi^{-p} \quad (5)$$

where M and $p(> 0)$ are constants. A graph plotted in Fig.1 clearly demonstrate the potential being shallow at late times, leading to acceleration. A review with explicit calculations for various potentials for the quintessence is found in [10].

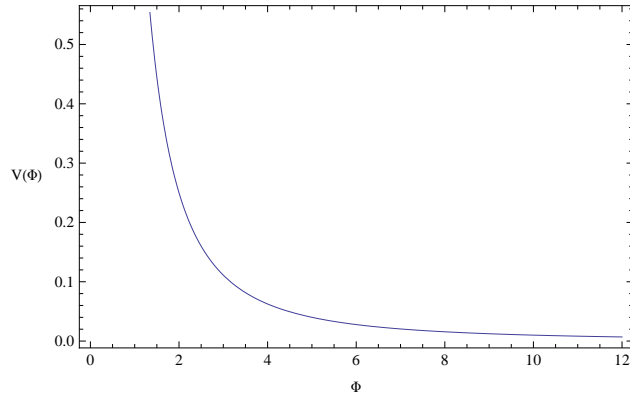


Figure 1. The figure shows $V(\Phi)$ vs Φ for the constants $M = 1$, $p = 2$

There are many works related to the quintessence model. We will present only a few here due to the large volume of existing work. Discussion about tracker solutions for conformally coupled quintessence model is discussed in [11]. Another article on tracking quintessence is written by Lola et.al [12]. Phase space analysis of quintessence fields trapped in a Randall-Sundrum Braneworld is done by Escobar et.al. [13]. Laboratory search for quintessence model is given in [14]. A study on quintessence and phantom dark energy from ghost D-branes is presented by Saridakis and Ward in [15].

The above discussion about the quintessence as a candidate for dark energy is from a cosmological point of view. Given the fact that black holes are a part of our cosmos, it is natural to ask how dark energy or quintessence in particular, affects the formation, evolution and physics of black holes in general. In an interesting article, Li and Wang [16] showed that black holes can exist in a Friedmann-Robertson-Walker universe dominated by dark energy. Ishwarchandra et.al. [17] produced an exact solution of a black hole in dark energy background with the state parameter $\omega = -\frac{1}{2}$. A detailed review of black holes in the presence of dark energy is given by Babichev et.al [18]. In this review wide range of field theoretical models were considered as dark energy.

In this paper we study how the quintessence effect the trajectories of massless particles around charged black holes. Studies of geodesics of massive and massless particles are one of the ways to understand the gravitational field around a black hole. Theoretical predictions related to geodesics such as gravitational lensing, perihelion shift, gravitational time delay and Lense-Thirring effect etc are aspects of black hole physics which can be compared to observations. From an astrophysical point of view,

the study of orbits of test particles are important to understand the flow of particles in accretion disks around black holes. Furthermore, circular orbits of photons (also known as “photon sphere” [19]) are important in studying the structure of the black hole geometry [20]. Also, quasinormal modes of black holes are related to null geodesics as shown in [21]. Hence studying null trajectories will help in understanding the stability properties of black holes to name a few applications. Considering all of above, we believe there is importance in doing a thorough understanding of trajectories in the presence of the dark energy element, quintessence.

In addition to the geodesics, we will address the issue of temperature of the black hole surrounded by dark energy. In a study of thermodynamics of dark energy, it was shown that the temperature of the universe filled with dark energy will increase [22]. In that study, the constituents of the dark energy were taken as massless bosons or fermions. With regard to black holes in this context, the question arises what would happen to the temperature of a black hole immersed in a universe with dark energy. We will address this in section 2 of this paper.

The paper is organized as follows: In section 2, an introduction to charged black holes surrounded by the quintessence is given. In section 3, null geodesics of the black hole is derived. In section 4, radial null geodesics are studied. In section 5, null geodesics with angular momentum are studied. In section 6, orbits of the photons corresponding to various values of the energy of photons is presented in detail. In section 7, the bending of light is presented. Finally, in section 8 the conclusion is given.

2 Charged black hole surrounded by the quintessence

In this section we will present the charged black hole surrounded by the quintessence studied in this paper. This particular black hole was derived by Kiselev [23]. Let us first present the action for the scalar field coupled to gravity and the Maxwell’s field as,

$$S = \frac{1}{16\pi} \int d^4x \sqrt{-g} \left(R - \frac{1}{2} \partial_\mu \Phi \partial^\mu \Phi - V(\Phi) - F_{\mu\nu} F^{\mu\nu} \right) \quad (6)$$

Here $F_{\mu\nu}$ represents the Maxwell’s field and R represents the curvature scalar. The quintessence field Φ has the action given by eq.(1). In cosmology, many potentials for the quintessence have been considered. Kiselev derived black hole solutions to the above action by adopting an unknown fluid with a particular type of energy momentum tensor. The adopted energy momentum tensor has a special property that it satisfies additive and linearity conditions. For a given state parameter ω , the energy momentum tensor was given as,

$$T_t^t = T_r^r = \rho_q \quad (7)$$

$$T_\theta^\theta = T_\phi^\phi = -\frac{1}{2} \rho_q (3\omega + 1) \quad (8)$$

where the density of quintessence matter, ρ_q is given by,

$$\rho_q = -\frac{\alpha}{2} \frac{3\omega}{r^{3(1+\omega)}} \quad (9)$$

For the range of $-1 < \omega < -\frac{1}{3}$, the universe with the quintessence will accelerate. General black hole solution for all ω were presented in [23]. In this paper, we pick $\omega = -\frac{2}{3}$ to facilitate computations. Hence, for this particular value of ω , the energy momentum tensor becomes,

$$T_t^t = T_r^r = \rho_q \quad (10)$$

$$T_\theta^\theta = T_\phi^\phi = \frac{1}{2}\rho_q \quad (11)$$

and the density of quintessence matter, ρ_q becomes

$$\rho_q = \frac{\alpha}{r} \quad (12)$$

The equation of state of the quintessence matter for the black hole is given by,

$$p_q = -\frac{2}{3}\rho_q \quad (13)$$

where p_q is the pressure. By solving the Einstein's equations with the energy momentum tensor for the quintessence matter and the Maxwell's field, one obtain the metric for static charged black hole solution with the quintessence as,

$$ds^2 = -f(r)dt^2 + \frac{dr^2}{f(r)} + r^2(d\theta^2 + \sin^2\theta d\phi^2) \quad (14)$$

where

$$f(r) = 1 - \frac{2M}{r} + \frac{Q^2}{r^2} - \alpha r \quad (15)$$

Here, M is the mass, Q is the charge, and α is a normalization factor related to the quintessence matter. This black hole is a special case of the class of black hole solutions derived by Kiselev [23]. As described by Kiselev [23], the pressure of the quintessence matter has to be negative to cause acceleration. Therefore matter energy density ρ_q is positive leading α to be positive.

There are few works related to the black hole described above. Thermodynamics of it has been studied in [24] [25] [26]. Quasinormal modes of the charged black hole surrounded by the quintessence has been studied in [27]. Null geodesics of the Schwarzschild black hole surrounded by the quintessence was studied by Fernando in [28]. The black hole solutions derived by Kiselev were extended to d dimensions by Chen et.al. [29]. They also studied Hawking radiation of the d -dimensional black holes.

2.1 Structure of horizons

In order to study the trajectories, one has to understand where the horizons are located for the given black hole. The horizons of the black hole is determined by the roots of the equation $f(r) = 0$, which leads to the cubic equation,

$$\alpha r^3 - r^2 + 2Mr - Q^2 = 0 \quad (16)$$

The nature of the roots of the polynomial in eq.(16) depends on the discriminant Δ given by,

$$\Delta = 4(M^2 - Q^2) + \alpha(-32M^3 + 36Q^2M) - 27\alpha^2Q^4 \quad (17)$$

When $\Delta > 0$, the polynomial will have three real roots. When $\Delta = 0$, there will be two real roots (degenerate root and a real root). When $\Delta < 0$ there will be only one real root. Hence, depending on the values of M , Q , and α , the black hole could have three, two or one horizon. A detailed discussion on how the roots behave when the parameters in the equation, M , Q and α are changed, are given in the paper by Fernando [26]. In Fig.2, a general class of plots for various values of the discriminant is given.

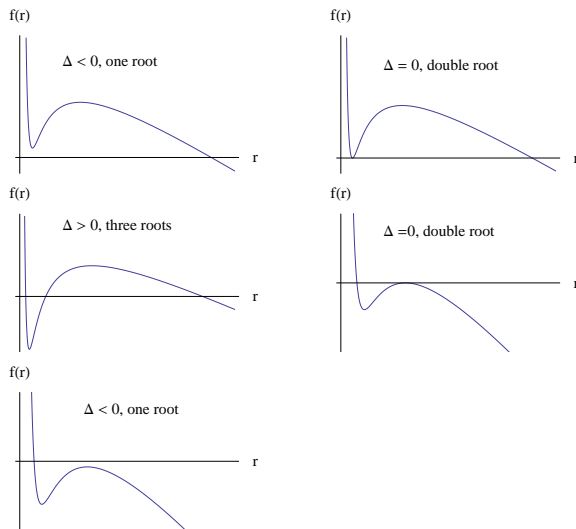


Figure 2. The figure shows $f(r)$ vs r for the black hole with the quintessence.

2.1.1 Three horizons

When there are three roots for $f(r)$, the smallest root represents the black hole inner horizon (r_+). The second root represents the black hole event horizon (r_{++}). The largest root corresponds to the cosmological horizon r_c which is similar to what is observed in Schwarzschild-de Sitter black hole [30]. For small α , $r_c \approx \frac{1}{\alpha}$ and $M \ll \frac{1}{\alpha}$.

The function $f(r)$ with three roots is given in Fig.3. There is a static region between r_{++} and r_c . In the rest of the paper, we will choose parameters where there are three horizons as in the Fig.3.

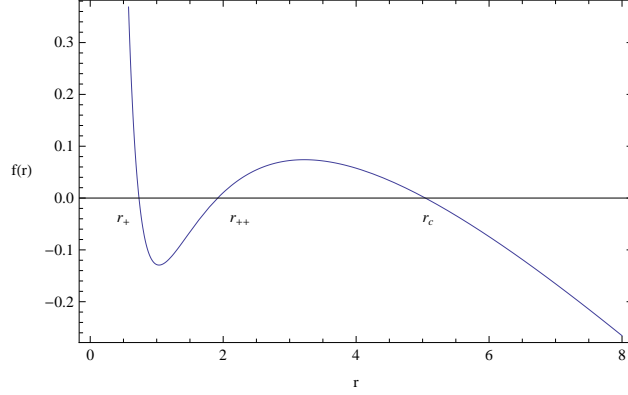


Figure 3. The figure shows $f(r)$ vs r for the black hole with $M = 0.96$, $Q = 0.96$ and $\alpha = 0.13$.

In the case of Fig.3, the three horizons are given by,

$$r_c = 2\sqrt{\frac{-\nu}{3}} \cos\left(\frac{\psi}{3}\right) + \frac{1}{3\alpha} \quad (18)$$

$$r_{++} = 2\sqrt{\frac{-\nu}{3}} \cos\left(\frac{\psi}{3} - \frac{2\pi}{3}\right) + \frac{1}{3\alpha} \quad (19)$$

$$r_+ = 2\sqrt{\frac{-\nu}{3}} \cos\left(\frac{\psi}{3} - \frac{\pi}{3}\right) + \frac{1}{3\alpha} \quad (20)$$

The three functions ν , σ and ψ are given by,

$$\nu = \frac{(6M\alpha - 1)}{3\alpha^2} \quad (21)$$

$$\sigma = \frac{(-2 + 18\alpha M - 27\alpha^2 Q^2)}{27\alpha^3} \quad (22)$$

$$\psi = \cos^{-1}\left(\frac{3\sigma}{2\nu} \sqrt{\frac{-3}{\nu}}\right) \quad (23)$$

2.1.2 Degenerate horizons

When $\Delta = 0$, and $(-1 + 6M\alpha) \neq 0$, there are double roots, and a simple root for the function $f(r)$. The double root, given by ρ , and the simple root, given by σ , are given by the following

$$\rho = \frac{(9\alpha Q^2 - 2M)}{2(-1 + 6M\alpha)} \quad (24)$$

$$\sigma = \frac{(-1 + 8\alpha M - 9\alpha^2 Q^2)}{\alpha(-1 + 6M\alpha)} \quad (25)$$

The corresponding function $f(r)$ for the extreme black hole is,

$$f(r) = \frac{\alpha(r - \rho)^2(\sigma - r)}{r^2} \quad (26)$$

When the function $\eta = -2 + 18\alpha M - 27\alpha^2 Q^2 > 0$, the double root corresponds to $r_{++} = r_c$ and the single root becomes r_+ . Such black holes are called ‘‘Nariai black holes’’. The function corresponding to such a situation is given in Fig.4. When $\eta = -2 + 18\alpha M - 27\alpha^2 Q^2 < 0$, the double root corresponds to $r_+ = r_{++}$ and the simple root becomes r_c . Such black holes are called ‘‘cold black holes’’. The function $f(r)$ for such a situation is given in Fig.5. It is also possible to have triple roots such that,

$$r_+ = r_{++} = r_c = \frac{1}{3\alpha} = \gamma \quad (27)$$

In this case, they are named ‘‘ultra cold black holes’’ and the function $f(r)$ takes the form,

$$f(r) = \frac{-\alpha(r - \gamma)^3}{r^2} \quad (28)$$

The function $f(r)$ corresponding to ultra cold black hole is given in Fig.6.

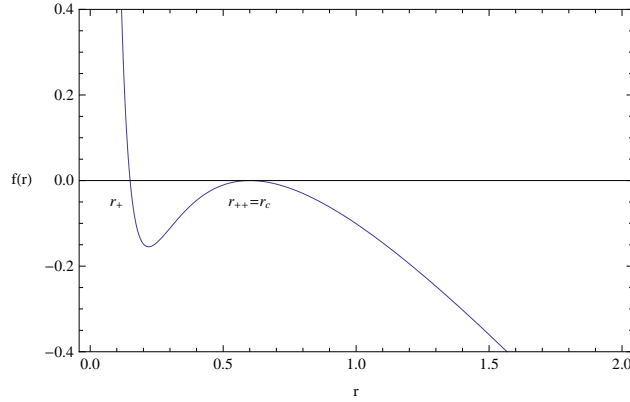


Figure 4. The figure shows $f(r)$ vs r for the Nariai black hole with $M = 0.2$, $Q = 0.2$ and $\alpha = 0.741$.

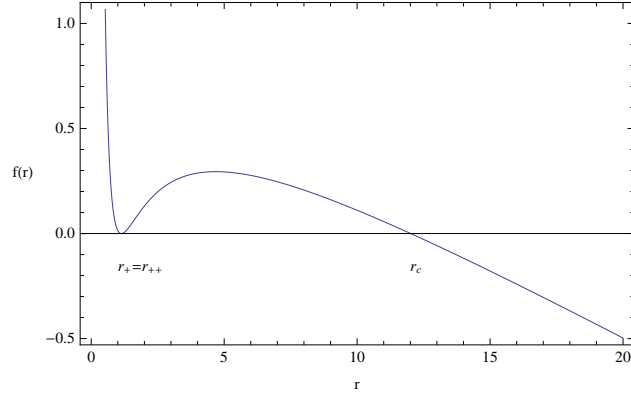


Figure 5. The figure shows $f(r)$ vs r for the cold black hole with $M = 1$, $Q = 1.041$ and $\alpha = 0.07$.

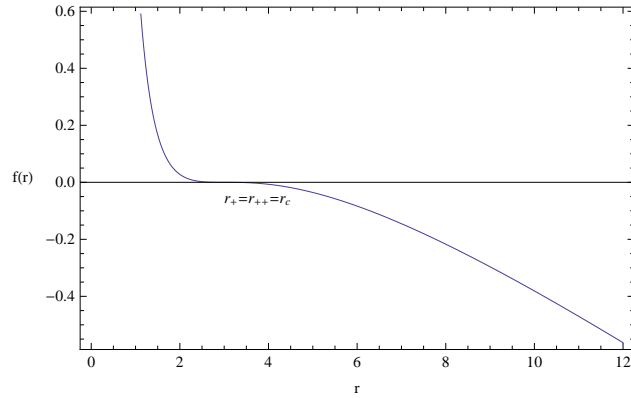


Figure 6. The figure shows $f(r)$ vs r for the ultra cold black hole with $M = 1.5$, $Q = 1.732$ and $\alpha = 0.11$.

2.2 Comparison of the charged black hole with the quintessence with Reissner-Nordstrom and Reissner-Nordstrom-de Sitter black hole

When there is cosmological constant present, the charged black hole solution is given by the Reissner-Nordstrom-de Sitter black hole [31]. When there is no dark energy, the corresponding charged black hole is given by the well known Reissner-Nordstrom black

hole. In this section we will compare the charged black hole with the quintessence to understand how their structure differs from each other.

The black hole without the quintessence, the Reissner-Nordstrom black hole, has the function $f(r)$,

$$f(r)_{RN} = 1 - \frac{2M}{r} + \frac{Q^2}{r^2} \quad (29)$$

The black hole with the cosmological constant, Reissner-Nordstrom-de Sitter black hole has the metric,

$$f(r)_{RNdeS} = 1 - \frac{2M}{r} + \frac{Q^2}{r^2} - \frac{\Lambda}{3} \quad (30)$$

In Fig.7, the function $f(r)$ is plotted for all three charged black holes. The Reissner-Nordstrom black hole is asymptotically flat while the other two are not. The Reissner-Nordstrom-de Sitter black hole is asymptotically de Sitter. It is clear that the Reissner-Nordstrom black hole has the smaller event horizon from all. Hence having a component of dark energy makes the black holes larger. Also, the quintessence black hole has a larger cosmological horizon.

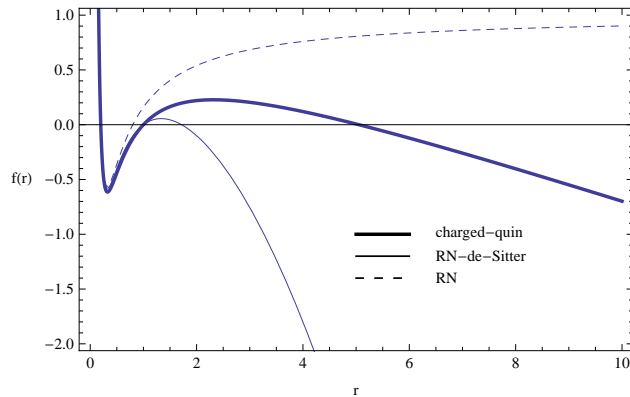


Figure 7. The figure shows $f(r)$ vs r for charged black hole with the quintessence, the Reissner-Nordstrom black hole and the Reissner-Nordstrom-de Sitter black holes. Here $M = 0.5$, $Q = 0.4$ and $\alpha = \frac{\Lambda}{3} = 0.16$

2.3 Temperature

Considering the black hole as a thermal system as first discovered by Hawking, it is important for us to understand the temperature of a black hole surrounded by quintessence field. The Hawking temperature of the charged black hole with the quintessence is given by,

$$T_H = \frac{1}{4\pi r_{++}} \left| 1 - \frac{Q^2}{r_{++}^2} - 2\alpha r_{++} \right| \quad (31)$$

In the Fig.8, the temperature is plotted as a function of α . The temperature increases when α increases to a maximum and decreases with further increasing α . If one compares the temperature with the charged black hole without the quintessence, then the one without is colder. As mentioned in the introduction, the temperature of the universe filled with dark energy increases [22]. It seems that the temperature of black holes also increase when immersed in a universe with dark energy. On the other hand, when mass of the black hole increases, the temperature of the black hole decreases as shown by Fig.10. This behavior is similar to the behavior of Reissner-Nordstrom and Reissner-Nordstrom-de Sitter black hole [26]. When the charge is increased, the temperature decreases and becomes zero as shown in Fig.9. What is happening is that the black hole is reaching the extreme condition when charge is increased leading to zero temperature. Such behavior is similar to what happens for Reissner-Nordstrom and Reissner-Nordstrom-de Sitter black holes.

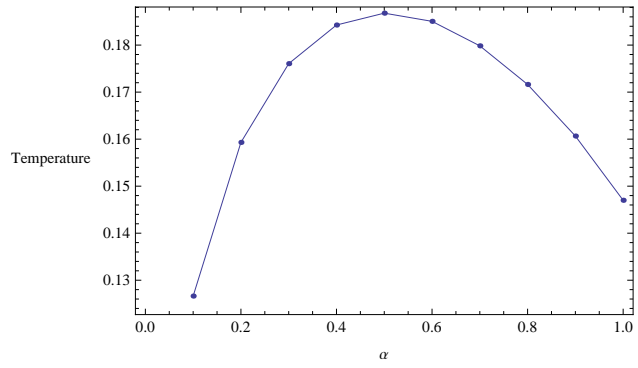


Figure 8. The figure shows $Temp$ vs α for the black hole with $M = 0.1$ and $Q = 0.1$.

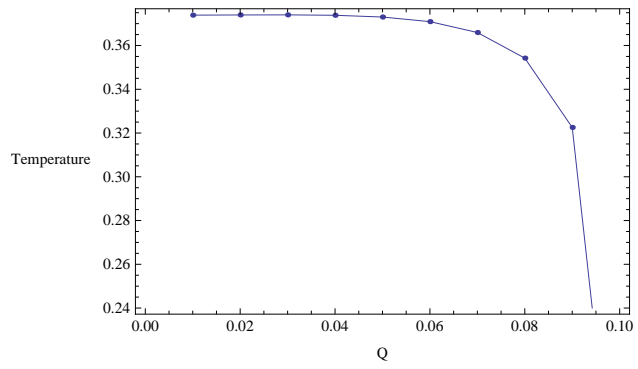


Figure 9. The figure shows $Temp$ vs Q for the black hole with $M = 0.1$ and $\alpha = 0.1$.

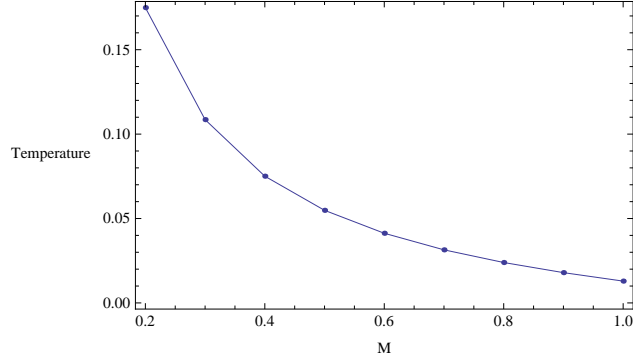


Figure 10. The figure shows $Temp$ vs M for the black hole with $Q = 0.1$ and $\alpha = 0.1$

2.3.1 Cold and ultra cold black holes with quintessence

It is well known that the charged black hole without the quintessence, Reissner-Nordstrom black hole, has zero temperature when it is extreme. Similarly, the charged black hole with the quintessence also has zero temperature configurations. Compared to the Reissner-Nordstrom black hole, there are two such cases: when the the black hole horizon and the inner horizon coincide, the temperature is zero and they are called “cold black holes”. On the other hand, when all three horizons coincide with $r_+ = r_{++} = r_c$, the black hole will have zero temperature and they are called “ultra cold black holes”. Cold and ultra cold black holes exists in Reissner-Nordstrom-de Sitter black hole which has a cosmological horizon. A detailed analysis of the temperature of such extreme black holes are discussed by one of the current authors, Fernando in [26].

3 Null geodesics of the black hole

In this section, we will derive the null geodesics for the charged black hole with the quintessence. The method used here is similar to the approach given in the well known book by Chandrasekhar [32]. The geodesics equations can be derived from the Lagrangian \mathcal{L} given by

$$\mathcal{L}_{geo} = -\frac{1}{2} \left(-f(r) \left(\frac{dt}{d\tau} \right)^2 + \frac{1}{f(r)} \left(\frac{dr}{d\tau} \right)^2 + r^2 \left(\frac{d\theta}{d\tau} \right)^2 + r^2 \sin^2 \theta \left(\frac{d\phi}{d\tau} \right)^2 \right) \quad (32)$$

where τ is an affine parameter along the geodesics. Due to the symmetries along t and ϕ directions, there are two conserved quantities of the photons given by E and

L . These two quantities are related to $f(r)$ as,

$$f(r)\dot{t} = E \quad (33)$$

$$r^2 \sin^2 \theta \dot{\phi} = L \quad (34)$$

In this paper the ‘‘dot’’ represents $\frac{d}{d\tau}$. We will consider the motion on the plane with $\theta = \frac{\pi}{2}$. Since the photon is confined to this plane, $\dot{\theta} = 0$ and $\ddot{\theta} = 0$. With \dot{t} and $\dot{\phi}$ given by eq.(33) and eq.(34), the Lagrangian in eq.(32) for photons becomes,

$$\dot{r}^2 + f(r) \frac{L^2}{r^2} = E^2 \quad (35)$$

One can define an effective potential $V_{eff} = \frac{L^2 f(r)}{r^2}$ for the motion of the photon as,

$$\dot{r}^2 + V_{eff} = E^2 \quad (36)$$

By combining eq(36) and eq.(34),

$$\frac{dr}{d\phi} = \frac{r^2}{L} \sqrt{E^2 - V_{eff}} \quad (37)$$

The effective potential V_{eff} can be expanded as,

$$V_{eff} = L^2 \frac{f(r)}{r^2} = \frac{L^2}{r^2} - \frac{2ML^2}{r^3} + \frac{Q^2 L^2}{r^4} - \frac{\alpha L^2}{r} \quad (38)$$

The first term represents the centrifugal potential. The second term corresponds to the relativistic correction due to general relativity. The third term is due to the fact that the black hole has electric charge. The last term is the one due to the quintessence scalar field around the charged black hole. One can see that it leads to an attractive term. Since the term due to the quintessence is negative, the potential is smaller compared to the one without the quintessence field. The potential does have a maximum and does not have a minimum. Hence, the photons do not have a stable circular orbits around the black hole. Since there is a maximum, the photons can have a unstable circular orbit. Various orbits for non-zero angular momentum will be discussed in section(5).

The effective potential is plotted in Fig.11. for various values of α . For large α , the maximum height is smaller. The potential is positive between the horizons since the zeros of the V_{eff} coincide with the two horizons, r_{++} and r_c . Therefore, as long as the two horizons are non-degenerate, the potential will be positive in the region considered. When the horizons degenerate, the maximum of the potential will be zero. If we further increase α (keeping M and Q constant), then the potential will become negative for all r values. In this paper we will only study the behavior of photons for non-degenerate horizons.

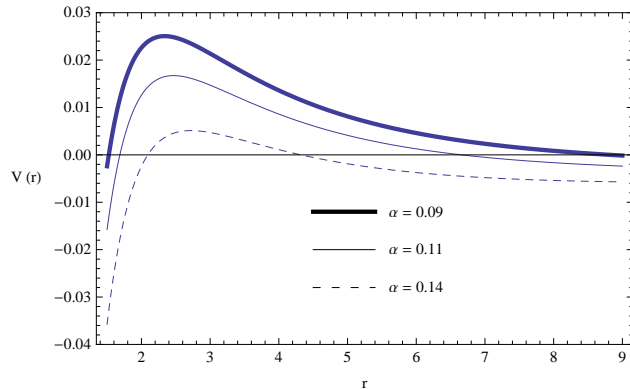


Figure 11. The figure shows V_{eff} vs r for the black hole with $M = 0.96, L = 1$ and $Q = 0.96$.

4 Radial null geodesics

First, we like to study the trajectories of photons without angular momentum. These trajectories lead to radial geodesics. This study is essential to understand what happens to a freely falling photon towards the two horizons, r_{++} and r_c . First let us focus on the space-time for which $f(r)$ has three real roots leading to non-degenerate horizons. For three real roots to exist, the discriminant given in eq.(17) has to be greater than zero.

If $f(r)$ has three real roots, then, $f(r)$ can be written as,

$$f(r) = -\alpha \frac{(r - r_+)(r - r_{++})(r - r_c)}{r^2} \quad (39)$$

For radial null geodesics, $L = 0$. Hence \dot{r} and \dot{t} are given by,

$$\dot{r} = \pm E \quad (40)$$

$$\dot{t} = \frac{E}{f(r)} \quad (41)$$

which leads to,

$$\frac{dt}{dr} = \pm \frac{1}{f(r)} = \pm \frac{1}{\left(1 - \frac{2M}{r} + \frac{Q^2}{r^2} - \alpha r\right)} \quad (42)$$

Before integrating the eq.(42), some clarification is needed. The “+” sign is chosen for the the outgoing photons which reach the cosmological horizon. The “-” sign is chosen for the ingoing photons which reach the event horizon at r_{++} . Hence there will be two solutions for time t as follows:

$$t(event - horizon) = \frac{1}{\alpha(r_+ - r_{++})(r_+ - r_c)(r_{++} - r_c)} \left(r_+^2(r_{++} - r_c) \text{Log}(r - r_+) + r_{++}^2(r_c - r_+) \text{Log}(r - r_{++}) + r_c^2(r_+ - r_{++}) \text{Log}(r - r_c) \right) + const_- \quad (43)$$

$$t(cosmological - horizon) = \frac{-1}{\alpha(r_+ - r_{++})(r_+ - r_c)(r_{++} - r_c)} \left(r_+^2(r_{++} - r_c) \text{Log}(r - r_+) + r_{++}^2(r_c - r_+) \text{Log}(r - r_{++}) + r_c^2(r_+ - r_{++}) \text{Log}(r - r_c) \right) + const_+ \quad (44)$$

The proper time can be obtained by integrating eq.(40). Once again, “-” sign corresponds to the time towards the even horizon and “+” sign corresponds to the time towards the cosmological horizon.

$$\tau(event - horizon) = -\frac{r}{E} + const_- \quad (45)$$

$$\tau(cosmological - horizon) = \frac{r}{E} + const_+ \quad (46)$$

When $r \rightarrow r_{++}, r_c$, time t goes to infinity as shown in Fig.13. The proper time is shown in Fig.12. and it is clear that it is finite when $r \rightarrow r_{++}, r_c$. It is interesting to observe the contrasting behavior of t and τ . What this implies physically is that for an observer stationary at a point in between the two horizons, a photon radially falling towards the horizons will take an infinite time to reach them. On the other hand, the photons, in its own proper time will reach the horizons at finite time.

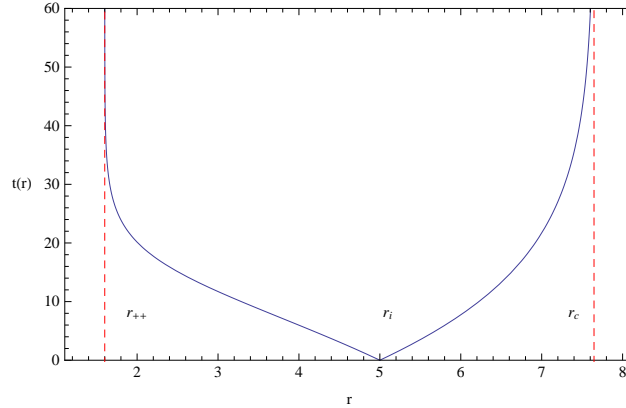


Figure 12. The figure shows t vs r for the black hole with $M = 0.96$, $Q = 0.96$. Here, $r = 5$ at $t = 0$.

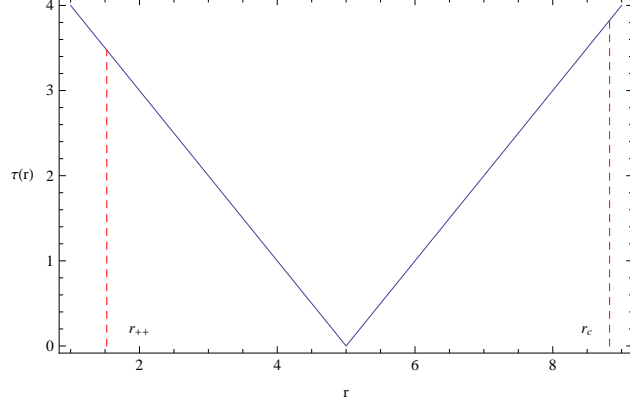


Figure 13. The figure shows τ vs r for the black hole with $M = 0.96$, $Q = 0.96$, $E = 1$ and $\alpha = 0.09$. Here, $r = 5$ at $\tau = 0$.

When the black hole becomes extreme, the horizons becomes degenerate with $r_{++} = r_c$. Lets call it ρ . In this case, $f(r)$ is given by the expression,

$$f(r) = -\frac{\alpha(r - r_+)(r - \rho)^2}{r^2} \quad (47)$$

Hence, for $r > \rho$, $f(r) < 0$. Therefore, r becomes a time coordinate and t becomes a spatial coordinate. The geodesics equations will be the same as before. The equation for the proper time will be the same and the solutions will be the same as in eq.(45) with the “-” sign in front. The reason to pick the “-” sign is due to the fact that for a photon falling towards the horizon from $r > \rho$, the proper time has to be positive. Once again, the proper time is finite for a in falling photon to reach the horizon. On the other hand, the time t can be obtained by integrating eq.(42) with the function $f(r)$ given in eq.(47). The solution is given by,

$$t = -\frac{\rho^2}{\alpha(r - \rho)(r_+ - \rho)} - \frac{\left(r_+^2 \text{Log}(r - r_+) + (\rho^2 - 2r_+\rho)\text{Log}(r - \rho)\right)}{(r_+ - \rho)^2} + \text{constant} \quad (48)$$

The integration constant is chosen such that $t = 0$ for $r = r_0 > \rho$. When $r \rightarrow \rho$, the time t reach $+\infty$. The “+” sign has to be picked from eq.(42) so that t increases when the photon falls towards the horizons.

5 Null geodesics with angular momentum

In this section, we will study the orbits for photons with non-zero angular momentum. Since $\dot{r}^2 + V_{eff} = E^2$, the motion of the particles will depend on the values of E . The effective potential for various values of E are plotted in Fig. 14. Three different scenarios depending on the values of E are discussed below.

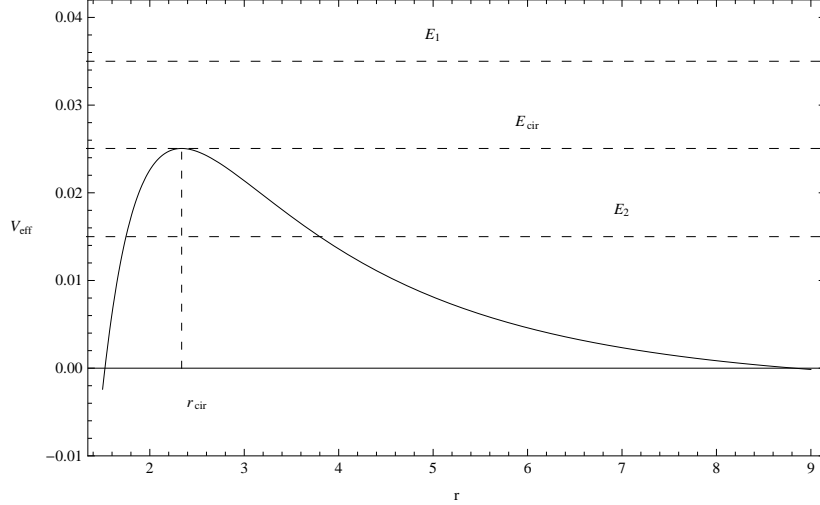


Figure 14. The figure shows V_{eff} vs r for the black hole with $M = 0.96$, $Q = 0.96$ and $\alpha = 0.09$.

$\mathbf{E = E_1}$:

In this case $E_1^2 - V_{eff} > 0$ for all r . Hence $\dot{r}^2 > 0$ for all r and a photon starting the motion at $r > r_{++}$ will fall into the black hole crossing the horizon.

$\mathbf{E = E_{cir}}$:

In this case, $\dot{r} = 0$ and the orbits are circular. These are unstable orbits which is evident from the nature of the potential.

$\mathbf{E = E_2}$:

In this case $\dot{r}^2 > 0$ only in two regions. If the initial position is far from the black hole, then the photon will have a turning point and will not fall into the black hole. If $r_{initial} < r_{cir}$, then the photon will fall into the black hole.

5.1 Circular orbits

From the plot for V_{eff} , it is clear that there is an unstable circular orbit. For circular orbits to occur, $E = E_{cir}$. At the circular orbits,

$$\frac{dV_{eff}}{dr} = 0 \quad (49)$$

which leads to,

$$\alpha r^3 - 2r^2 + 6Mr - 4Q^2 = 0 \quad (50)$$

Equation (50) is a cubic equation which has three roots. By observing the behavior of the potential by means of graphical presentation, we conclude that the root

corresponding to the unstable circular orbit is the second root given by,

$$r_{cir} = 2\sqrt{\frac{-\nu_1}{3}} \cos\left(\frac{\psi_1}{3} - \frac{2\pi}{3}\right) + \frac{2}{3\alpha} \quad (51)$$

where,

$$\nu_1 = \frac{(-4 + 18\alpha M)}{3\alpha^2} \quad (52)$$

$$\sigma_1 = \frac{(-16 + 108\alpha M - 108\alpha^2 Q^2)}{27\alpha^3} \quad (53)$$

$$\psi_1 = \cos^{-1}\left(\frac{3\sigma_1}{2\nu_1} \sqrt{\frac{-3}{\nu_1}}\right) \quad (54)$$

In Fig.15, r_{cir} is plotted with α . From the figure, the radius of the circular orbit with the quintessence is larger. In Fig. 16, radius of the circular orbit is plotted as a function of Q . When charge increases, r_{cir} decreases.

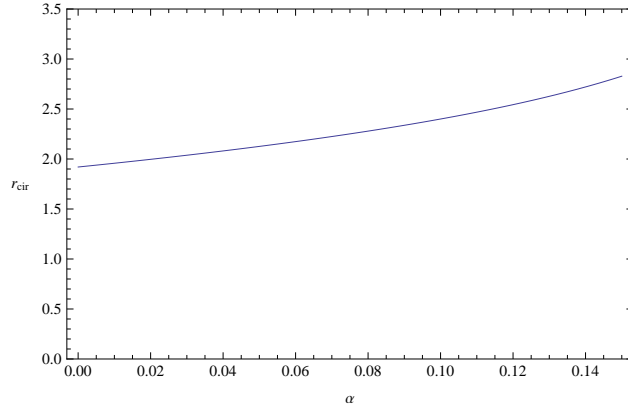


Figure 15. The figure shows r_{cir} vs α for the black hole with $M = 0.96$, and $Q = 0.96$.

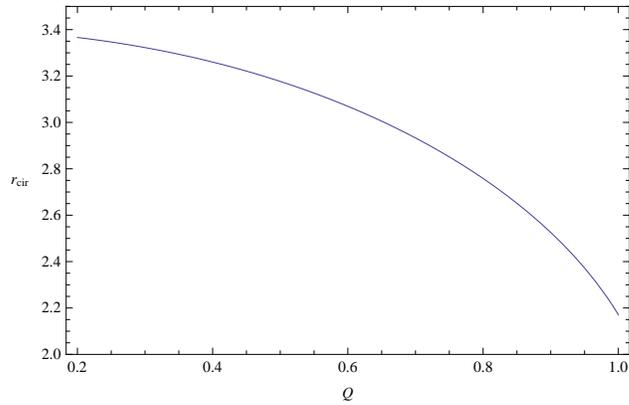


Figure 16. The figure shows r_{cir} vs Q for the black hole with $M = 0.96$, and $\alpha = 0.09$.

The circular orbit at $r = r_{cir}$ is called the ‘‘photon sphere’’ [19]. r_{cir} is independent of E and L . One must note that at the circular orbit, the following condition is also true.

$$V_{eff} = E_{cir}^2 \quad (55)$$

From eq.(55),

$$\frac{E_{cir}^2}{L_{cir}^2} = \frac{f(r_{cir})}{r_{cir}^2} \Rightarrow \frac{1}{D_{cir}^2} = \frac{Q^2}{r_{cir}^4} - \frac{2M}{r_{cir}^3} + \frac{1}{r_{cir}^2} - \frac{\alpha}{r_{cir}} \quad (56)$$

D_{cir} is the critical impact parameter given by $\frac{L_{cir}}{E_{cir}}$. In Fig.17, D_{cir} is plotted as a function of α . D_{cir} increases with α . Hence the black hole surrounded by dark energy requires higher impact parameter to orbit in a circle around the black hole. Also, for fixed value of L_{cir} , E_{cir} decreases when α increases. Hence, photons needs less energy to go in circular orbits for higher α . As a consequence, the value of E_1 and E_2 also decrease for higher α .

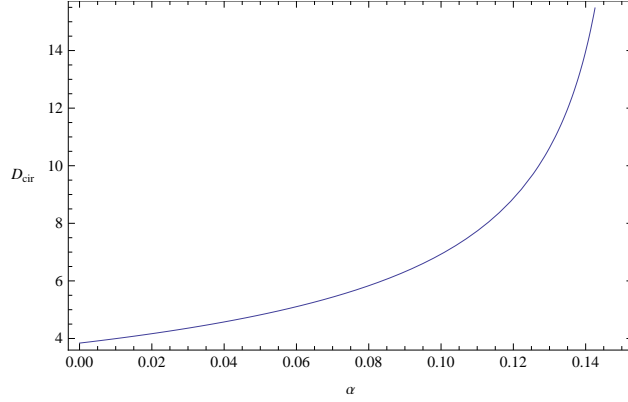


Figure 17. The figure shows D_{cir} vs α for a black hole with $M = 0.96$, and $Q = 0.96$.

When $\alpha = 0$, the geometry becomes the Reissner-Nordstrom black hole. It also has an unstable circular orbit and it is at,

$$r_{cir}^{RN} = \frac{1}{2} \left(3M + \sqrt{9M^2 - 8Q^2} \right) \quad (57)$$

The null geodesics of the Reissner-Nordstrom black hole is well studied by Chandrasekhar in [32].

6 Geodesics with the variable u

One can do the well know change of variable, $u = \frac{1}{r}$ to study the orbits. First, one can rewrite the eq.(37) as,

$$\left(\frac{du}{d\phi}\right)^2 = g(u) \quad (58)$$

where,

$$g(u) = 2Mu^3 - u^2 + \alpha u + \frac{E^2}{L^2} - Q^2u^4 \quad (59)$$

The geometry of the geodesics will depend on the roots of the function $g(u)$. Notice that when $u \rightarrow \pm\infty$, $g(u) \rightarrow -\infty$. Also, when $u \rightarrow 0$, $g(u) \rightarrow \frac{E^2}{L^2}$. Therefore, $g(u)$ always have two real roots and one of them is negative and the other a positive one. Since $g(u)$ is a polynomial of fourth order, it is possible for $g(u)$ to have two more real roots or a complex conjugate pair. It is also possible for $g(u)$ to have degenerate roots. All these possibilities are shown in Fig.18.

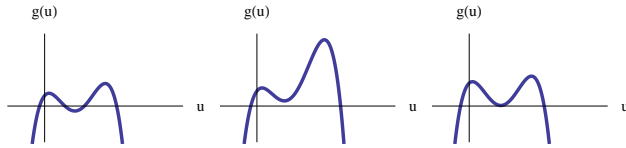


Figure 18. The graph shows the function $g(u)$ as a function of u .

It is interesting to compare the root structure with the Reissner-Nordstrom black hole which is the charged black hole without the quintessence ($\alpha = 0$). In that case,

$$g_{RN}(u) = 2Mu^3 - u^2 + \frac{E^2}{L^2} - Q^2u^4 \quad (60)$$

The root structure is very similar to the one with the quintessence.

6.1 General solution for ϕ in terms of u (or r)

In this section, we will present solutions to ϕ in terms of u .

From eq.(58),

$$\left(\frac{du}{d\phi}\right) = \pm\sqrt{g(u)} \quad (61)$$

where $g(u)$ is written as,

$$g(u) = -Q^2(u - u_1)(u - u_2)(u - u_3)(u - u_4) \quad (62)$$

Here, the “+” sign will be chosen without lose of generality. When the above equation is integrated, a relation between u and ϕ in terms of Jacobi-elliptic integral $\mathcal{F}(\xi, y)$ is obtained as,

$$\phi = \frac{2}{Q} \frac{\mathcal{F}(\xi, y)}{\sqrt{(u_2 - u_3)(u_1 - u_4)}} + \text{constant} \quad (63)$$

Here,

$$\sin \xi = \sqrt{\frac{(u - u_2)(u_1 - u_4)}{(u - u_1)(u_2 - u_4)}} \quad (64)$$

$$y = \frac{(u_1 - u_3)(u_2 - u_4)}{(u_2 - u_3)(u_1 - u_4)} \quad (65)$$

$$\mathcal{F}(\xi, y) = \int_0^\xi \frac{d\lambda}{\sqrt{1 - y \sin^2(\lambda)}} \quad (66)$$

The constant in the equation for ϕ is an integration constant and could be complex depending on the values of the roots. However, the final result for ϕ will be real.

6.2 Orbits for various values of energy E

Depending on the values of E, M, Q, α and L , the root structure of $g(u)$ varies. In the following, we will highlight separate cases.

$E > E_{\text{cir}}$:

In this case, the plot of $g(u)$ is given in Fig.19. The corresponding orbits for two values of energy E is given in the Fig.20. The one with less energy falls into the black hole earlier than the one with more energy as expected.

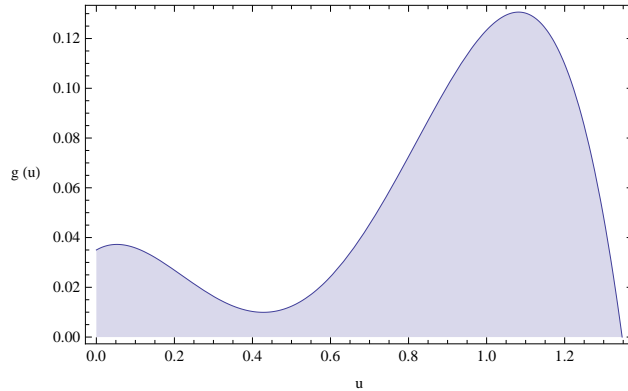


Figure 19. The graph shows the function $g(u)$ as a function of u . Here, $M = 0.96, Q = 0.96, L = 1, \alpha = 0.09$ and $E = 0.187$.

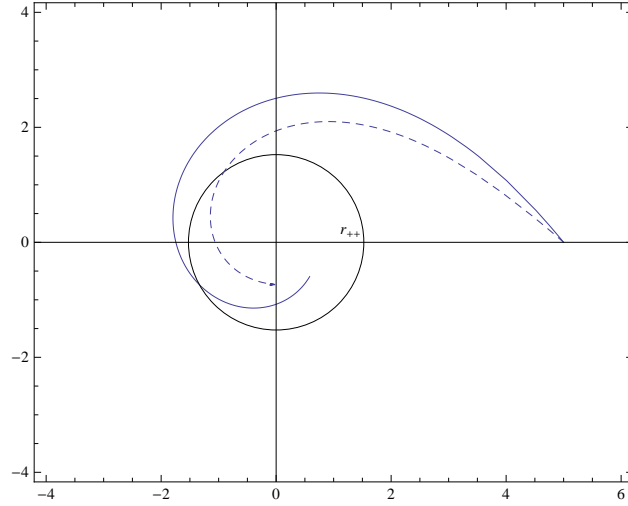


Figure 20. The graph shows the polar plot of ϕ of the particle with energies $E = 0.187$ (thick) and $E = 0.247$ (dashed). The black hole has $M = 0.96, Q = 0.96, L = 1$, and $\alpha = 0.09$. The circle is the black hole horizon.

$$\mathbf{E} = \mathbf{E}_{\text{cir}}:$$

In this case, the plot of $g(u)$ is given in Fig.21. The corresponding orbit is given in Fig.22. There are two orbits with one starting inside the black hole and the other starting out side the black hole. Since they both have the same critical energy, E_{cir} , they both reach the unstable circular orbit at $r = r_{\text{cir}}$.

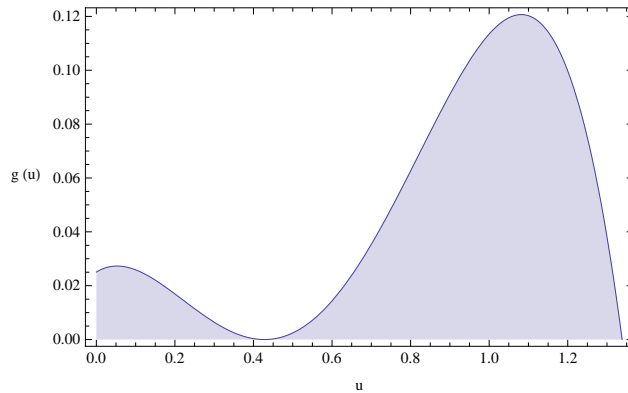


Figure 21. The graph shows the function $g(u)$ as a function of u . Here, $M = 0.96, Q = 0.96, L = 1, \alpha = 0.09$ and $E = 0.158$

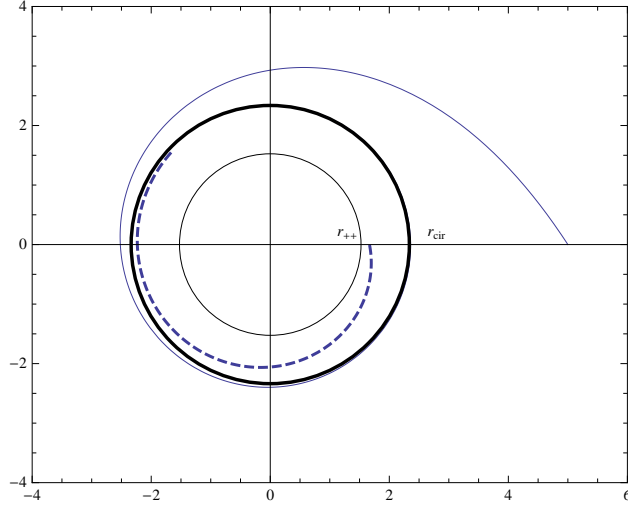


Figure 22. The graph shows the polar plot of ϕ of the particle with $E = 0.158$. The black hole has $M = 0.96, Q = 0.96, L = 1$ and $\alpha = 0.09$. The trajectory from out side approaches the black hole and merge to the circular orbit at $r = r_{cir}$. The trajectory from inside given by the dashed curve approaches the circular orbit from inside and merge the circular orbit at $r = r_{cir}$ as expected.

$E < E_{cir}$:

In this case, the plot of $g(u)$ is given in Fig.23. The corresponding orbit is given in Fig.24. There are two orbits in the Fig.24. One with low energy (thick curve) and the one with high energy(dashed curve). The one with the high energy do not bend as much as the one with lower energy in its orbit as expected.

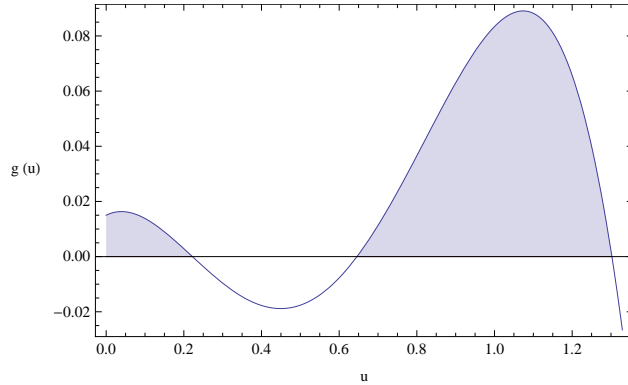


Figure 23. The graph shows the function $g(u)$ as a function of u . Here, $M = 0.96, Q = 0.96, L = 1, \alpha = 0.07$ and $E = 0.122$

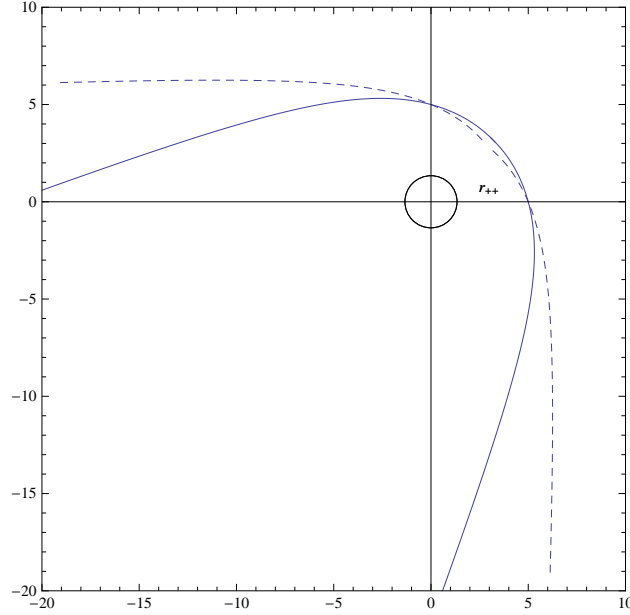


Figure 24. The graph shows the polar plots of ϕ of the particle with energies $E = 0.122$ (thick) and $E = 0.138$ (dashed). The black hole has $M = 0.96, Q = 0.96, L = 1, \alpha = 0.07$

7 Bending of light

When photons travel around a black hole, the light bends. This deflection of light is one of the few observational tools available to study the geometry around a black hole or an object with strong gravitational field. There are many works in the literature with focus on bending of light around black holes. We will mention only a few that may be related to the present work. The deflection of light and the gravitational frequency shift of the Schwarzschild black hole surrounded by the quintessence was studied by Liu et.al [33]. Light bending as a probe of the dark energy was presented by Finelli et.al. in [34]. Bending of light in conformal gravity was presented in [35]. Bending of light and the motion of particles in the background of the Schwarzschild-de Sitter black hole is well studied by many authors: bending of light is studied by Ishak et.al. [36], and gravitational lensing has been studied by Schücker [37] and Sereno [38]. A comprehensive study of motion of particles around the Schwarzschild-de Sitter black hole was done by Struchlik [39]. Properties of the motion of massive particles and photons around the Reissner-Nordstrom-de Sitter black holes was studied by Stuchlik and Hledik in [40].

The conventional approach of calculating the angle of deflection gives it as [41],

$$\Delta \varphi = 2|\phi(\infty) - \phi(r_o)| - \pi \quad (67)$$

where r_o is the closest approach of the photon when it travels around the black hole. However, this approach works only for asymptotically flat space-times. In the current work, the space-time is asymptotically non-flat and $r \rightarrow \infty$ does not make sense. To remedy this situation, Rindler and Ishak developed a method to find the bending angle in asymptotically non-flat space-times [42].

In particular, they applied this approach to find the bending angle of Schwarzschild-de Sitter black hole to find the contribution of the cosmological constant on the bending angle. Here, we will follow their approach to compute the bending angle for the charged black hole with the quintessence.

7.1 Rindler Ishak method to find the angle of deflection

Rindler-Ishak method is based on the Figure. 25. They defined the general bending angle as $\epsilon = \psi - \phi$. Hence, the total bending angle was defined as 2ϵ when $\phi = 0$, which gives $2\epsilon_0 = 2\psi_0$. The angle ψ is given by,

$$\tan\psi = \frac{\sqrt{f(r)}r}{|A|} \quad (68)$$

where

$$A = \frac{dr}{d\phi} \quad (69)$$

For more details on the derivation of equation (68), the reader is referred to the paper by Rindler and Ishak [42].

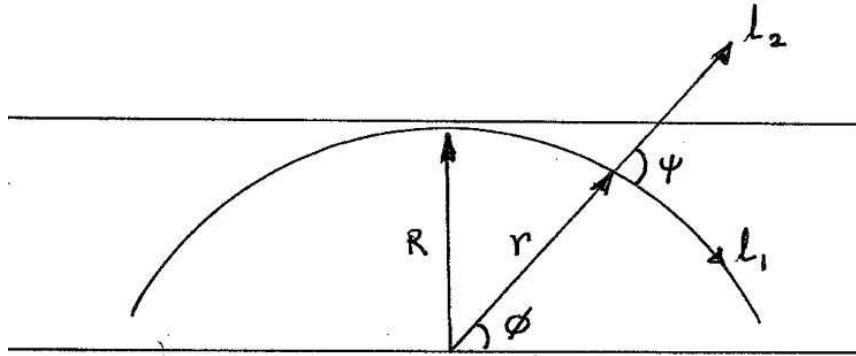


Figure 25. The figure shows a light ray bending around the black hole.

7.2 Perturbative approach to find $u = \frac{1}{r}$ as a function of ϕ .

In this section we will present how we found a solution for u in terms of ϕ using a perturbative approach. From equation(58), which corresponds to the photon path around the black hole, one can obtain a second order differential equation,

$$\frac{d^2u}{d\phi^2} + u - \frac{\alpha}{2} = 3Mu^2 - 2Q^2u^3 \quad (70)$$

This is a non-linear differential equation which can be solved perturbatively in powers of M and Q^2 . Let the solution for $M = 0, Q = 0$ be u_0 and a small perturbation be u_1 . Hence to first order, $u = u_0 + u_1$. By substituting this to the equation (70), we get two equation,

$$\frac{d^2u_0}{d\phi^2} + u_0 - \frac{\alpha}{2} = 0 \quad (71)$$

and,

$$\frac{d^2u_1}{d\phi^2} + u_1 = 3Mu_0^2 - 2Q^2u_0^3 \quad (72)$$

First, let us solve the zeroth order equation given by,

$$\frac{d^2u_0}{d\phi^2} + u_0 - \frac{\alpha}{2} = 0 \quad (73)$$

Let $\bar{u} = u - \alpha/2$. Then, equation(73) simplifies into,

$$\frac{d^2\bar{u}_0}{d\phi^2} + \bar{u}_0 = 0 \quad (74)$$

The solution to equation(74) is,

$$\bar{u} = \frac{\cos\phi}{R} \quad (75)$$

R is a constant which appears in Figure.25. Hence the solution for u_0 is,

$$u_0 = \frac{\cos\phi}{R} + \frac{\alpha}{2} \quad (76)$$

Now, the solution for u_0 can be substituted to the right hand of the first order equation(72) leading to,

$$\frac{d^2u_1}{d\phi^2} + u_1 = 3M \left(\frac{\cos\phi}{R} + \frac{\alpha}{2} \right)^2 - 2Q^2 \left(\frac{\cos\phi}{R} + \frac{\alpha}{2} \right)^3 \quad (77)$$

The final solution $u = u_0 + u_1$. Replace ϕ with $(\pi/2 - \phi)$ to reflect the angles in Figure 25. Then, the solution u is given by,

$$u = \frac{\alpha}{2} + \frac{3M\alpha^2}{4} - \frac{Q^2\alpha^3}{4} + \frac{B_1}{R} + \frac{B_2}{R^2} + \frac{B_3}{R^3} \quad (78)$$

where,

$$B_1 = \sin\phi + M \left(\frac{3\alpha\pi}{4} \cos\phi - \frac{3}{2} \phi \alpha \cos\phi + \frac{3}{2} \alpha \sin\phi \right) + Q^2 \left(-\frac{3}{8} \pi \alpha^2 \cos\phi + \frac{3}{4} \phi \alpha^2 \cos\phi - \frac{3}{4} \alpha^2 \sin\phi \right) \quad (79)$$

$$B_2 = M \left(\frac{3}{2} + \frac{1}{2} \cos 2\phi \right) + Q^2 \left(-\frac{3\alpha}{2} - \frac{\alpha}{2} \cos 2\phi \right) \quad (80)$$

$$B_3 = Q^2 \left(-\frac{3}{8} \pi \cos\phi + \frac{3}{4} \phi \cos\phi - \frac{9}{16} \sin\phi - \frac{1}{16} \sin 3\phi \right) \quad (81)$$

When $\alpha \rightarrow 0$ and $Q \rightarrow 0$, one obtain,

$$u = \frac{\sin\phi}{R} + \frac{M}{2R^2} (3 + \cos 2\phi) \quad (82)$$

which is the u value obtained by Rindler and Ishak [42] for the Schwarzschild-de Sitter black hole.

Now in order to find the bending angle, one can use the fact that $r = \frac{1}{u}$ and let $\phi = 0$ to obtain

$$r(\phi = 0) = r_z = \frac{8R^3}{X} \quad (83)$$

and

$$A = \frac{dr}{d\phi}(\phi = 0) = \frac{-64R^5}{X^2} \quad (84)$$

where,

$$X = -3\pi \left(-2MR^2\alpha + Q^2(1 + R^2\alpha^2) \right) + 2R \left(M(8 + 3R^2\alpha^2) - \alpha(-2R^2 + Q^2(8 + R^2\alpha^2)) \right) \quad (85)$$

Now, one can utilize the equation (68) to find the bending angle ψ_0 .

$$\tan\psi = \sqrt{f(r_{\phi=0})} \frac{|X|}{8R^2} \quad (86)$$

We have taken the absolute value of X since one has to have the absolute value of A in the expression. Now, we will expand \sqrt{f} for small values of M/R , Q^2/R , αR and substitute r_z for r leading to,

$$\sqrt{f} \approx 1 - \frac{M}{r_z} + \frac{Q^2}{2r_z^2} - \frac{\alpha r_z}{2} \quad (87)$$

Also, we will assume that the angle ψ is small. Hence $\tan\psi \approx \psi$. Hence the angle ψ at $\phi = 0$, which is ψ_0 is,

$$\psi_0 \approx \left(1 - \frac{M}{r_z} + \frac{Q^2}{2r_z^2} - \frac{\alpha r_z}{2} \right) \frac{|X|}{8R^2} \quad (88)$$

By substituting X and r_z into the above expression and expanding for small M/R , Q^2/R^2 , and αR , we obtain ψ_0 . Therefore, the bending angle, $2\psi_0$ is given by,

$$2\psi_0 = \frac{4M}{R} + \frac{3\pi M\alpha}{2} - \frac{4M^2\alpha}{R} - \frac{3\pi Q^2}{4R^2} - \frac{4Q^2\alpha}{R} + \frac{3\pi M^2 Q^2}{2R^4} \quad (89)$$

Notice that the first term is the one for Schwarzschild black hole. Other terms are corrections due to α and Q^2 . We have omitted higher order terms here. Another work which has followed Rindler and Ishak method to compute bending angle is given in [43].

8 Conclusion

The objective of this paper is to study a black hole surrounded by a scalar field called “quintessence.” The quintessence field is one of possible sources for dark energy considered in research currently. Our main goal in this paper was to study null trajectories around a charged black hole surrounded by the quintessence derived by Kiselev [23].

First we presented the structure of horizons where it was shown that the black hole can have three, two or one horizons. In contrast, the charged black hole without the quintessence can have only two or one horizon. When compared with the Reissner-Nordstrom-de Sitter black hole, the one with the quintessence also has a cosmological horizon. We observed that the black holes with a dark energy component have a larger event horizon. The black hole with the quintessence has higher temperature compared to the one without. However, they also have zero temperature configurations named, cold and ultra cold black holes.

To understand the trajectories, we did a detailed study of null geodesics around the charged black hole surrounded by quintessence. Both radial and the trajectories with angular momentum are studied. The exact solution to the geodesics equation with angular momentum is obtained in terms of Jacobi-elliptic integrals. The orbits for various values of the energy are presented. The circular orbits were studied in detail which were unstable. The radius of the circular orbits were larger for large α and small for large Q .

As an application of the photon trajectories, we have also studied the bending angle of light. We have used a method developed by Rindler and Ishak [42]. First we used a perturbative approach to obtain the solutions for the trajectory. Then we used expansions around small M/R , Q^2/R^2 and αR , to obtain the bending angle.

In this paper we have focused on the photon motion for black holes with non-degenerate horizons. The geodesics for the extreme black holes and the global structure of the extreme black holes would be an interesting avenue to study. For example, the structure of the extreme Schwarzschild-de Sitter space-time is studied by Podolsky in [44]. We are planning on reporting on the extreme charged black hole with quintessence in the future.

It would also be interesting to do further analysis of strong gravitational lensing along the lines of the work done by Virbhadra et.al [45].

References

- [1] S. Perlmutter et. al., *Measurements of Ω and Λ from 42 high-redshift supernovae*, *Astrophys. J.* **517** 565 (1999)
- [2] A.G. Riess et. al., *Observational Evidence from Supernovae for an Accelerating Universe and a Cosmological Constant*, *Astron. J.* **116** 1009 (1998); *BVRI Light Curves for 22 Type Ia Supernovae*, *Astron. J.* **117** 707(1999)
- [3] P. J. E. Peebles, & B. Ratra, *The cosmological constant and dark energy*, *Rev. Mod. Phys.* **75** 559 (2003)
- [4] N. Radicella, & D. Pavion, *A thermodynamic motivation for dark energy*, *Gen. Rel. Grav.* **44** 685 (2012)
- [5] Y. Wang & P. Mukherjee, *Observational constraints on dark energy and cosmic curvature*, *Phys. Rev.* **D76** 103533 (2007)
- [6] A. F. Heavens, T. D. Kitching, & A. N. Taylor, *Measuring dark energy properties with 3D cosmic shera*, *Mon. Not. Roy. Astron. Soc.* **373**, 105 (2006)
- [7] A. Refregier et. al. *DUNE: The Dark Universe Explorer*, astro-ph/0610062
- [8] S. Weinberg, *Rev. Mod. Phys.* **61** 1 (1989)
- [9] E. J. Copeland, M. Sami & S. Tsujikawa., *Dynamics of Dark energy*, *Int. Jour. Modern. Phys.* **D15** 1753 (2006)
- [10] S. Tsujikawa, *Quintessence: A review*, *Class. Quant. Grav.* **30** 214003 (2013)
- [11] F. Shojai, R. Moti, & F. Najdat, *Tracker coupled quintessence* , *Phys. Rev.* **D87** 043007 (2013)
- [12] S. Lola, C. Pallis, & E. Tzelati, *Tracking quintessence and cold dark matter candidates*, *JCAP* 0911: 017 (2009)
- [13] D. Escobar, C. R. Fadrugas, G. Leon, & Y. Leyva, *Phase space analysis of quintessence fields in Randall-Sundrum Braneworld: a refined study*, *Class. Quant. Grav.* **29** 175005 (2012)
- [14] M.V. Romalis & R.R. Caldwell, *Laboratory search for a quintessence field*, arXiv:1302.1579

- [15] E. N. Saridakis & J. Ward, *Quintessence and phantom dark energy from ghost D-branes*, Phys. Rev. **D 80** 083003 (2009)
- [16] Z Li & A. Wang, *Existence of black holes in Friedmann-Robertson-Walker universe dominated by dark energy*, Mod. Phys. Lett. **A 22** 1663 (2007)
- [17] N. Ishwarchandra, N. Ibohal, & K. Y. Singh, *Schwarzschild black hole in dark energy background*, Astro. and Space. Sci. **353** 633 (2014)
- [18] E. O. Babichev, V. I. Dokuchaev & Y. N. Eroshenko, *Black holes in the presence of dark energy*, Phys.-Usp. **56**, 1155 (2013); Uspekhi Fiz. Nauk **183**, 1257 (2013)
- [19] C.M. Claudel, K.S. Virbhadra & G. F. R. Ellis, *The geometry of photon spheres*, J. Math. Phys. **42** (2001) 818
- [20] S. Hod, *Hairy black holes and null circular geodesics*, Phy. Rev. **D 84** 124030 (2011)
- [21] V. Cardoso, A.S. Miranda, E. Berti, H. Witek & V.T. Zanchin, *Geodesics stability, Lyapunov exponents and quasinormal modes*, Phys.Rev. **D79** 064016 (2009)
- [22] J. A. S. Lima & J. S. Alcaniz, *Thermodynamics, spectral distribution and nature of dark energy*, Phys. Lett. **B600** 191, (2004)
- [23] V.V. Kiselev, *Quintessence and black holes*, Class. Quant. Grav. **20** 1187 (2003)
- [24] B.B. Thomas, M. Saleh & T.C. Kofane, *Thermodynamics and phase transition of the Reissner-Nordstrom black hole surrounded by quintessence*, Gen. Rel. Grav. **44** 2181 (2012)
- [25] M. Azreg-Ainou & M.E. Rodrigues, *Thermodynamical, geometrical and Poincare methods for charged black holes in presence of quintessence*, arXiv:1211.5909
- [26] S. Fernando, *Cold, ultracold and Nariai black holes with quintessence*, Gen. Rel. Grav. **45** 2053 (2013)
- [27] N. Varghese & V.C. Kuriakose, *Massive charged scalar quasinormal modes of Reissner-Nordstrom black hole surrounded by quintessence*, Gen. Rel. Grav. **41** 1249 (2009)
- [28] S. Fernando, *Schwarzschild black hole surrounded by quintessence: null geodesics*, Gen. Rel. Grav. **44** 1857 (2012)
- [29] S. Chen, B. Wang, & R. Su, *Hawking radiation in d-dimensional static spherically-symmetric black hole surrounded by quintessence* Phys. Rev. **D77** 124011 (2008)

- [30] M. Brum & S. E. Joras, *Hadamard state in Schwarzschild-de Sitter space-time*, arXiv:1405.7916
- [31] H. Laue & M. Weiss, *Maximally extended Reissner-Nordstrom manifold with cosmological constant*, Phys. Rev. **D 16** 3376 (1977)
- [32] S. Chandrasekhar, *The Mathematical Theory of Black holes*, Oxford, UK:
- [33] M. Liu, J. Liu & Y. Gui, *The influence of free quintessence on gravitational frequency shift and deflection of light with 4D momentum*, Eur. Phys. J. **C 59** 107 (2009)
- [34] F. Finelli, M. Galaverni, & A. Gruppuso, *Light bending as a probe of the nature of dark energy*, Phys. Rev. **D 75** 043003, (2007)
- [35] J. Sultana & D. Kazanas, *Bending of light in conformal Weyl gravity*, Phys. Rev. **D 81** 127502 (2010).
- [36] M. Ishak, W. Rindler, J. Dossett, J. Moldenhauer & C. Allison, *A new independent limit on the cosmological constant/dark energy from the relativistic bending of light by galaxies and clusters of galaxies*, Mon. Not. R. Astron. Soc. **388**, 1279-1283 (2008)
- [37] T. Schucker, *Lensing in an interior Kottler solution*, Gen. Rel. Grav. **42** 1991-1995 (2010)
- [38] M. Sereno, *Role of Λ in the cosmological lens equation*, Phy. Rev. Lett. **102** 021301 (2009)
- [39] Z. Stuchlik, *The motion of test particles in black-hole backgrounds with non-zero cosmological constant*, Bull. Astron. Institutes. Czechoslovakia, **34** 129-149 (1983)
- [40] Z. Stucklik & S. Hledik, *Properties of the Reissner-Nordstrom space-times with a nonzero cosmological constant*, Acta Physica Solvaca **52** 363-407 (2002)
- [41] S. Weinberg, *Gravitation and Cosmology*, John Wiley and Sons, Inc., (1972)
- [42] M. Ishak & W. Rindler, *Contribution of the cosmological constant to the relativistic bending of light revisited*, Phys. Rev. **D 76**, 043006 (2007)
- [43] C. Cattano, M. Scalia, E. Laserra & I. Bochicchio, *Correct Weyl deflection in Weyl conformal gravity*, Phys. Rev. **D 87** 047503 (2013)
- [44] J. Podolsky, *The structure of the extreme Schwarzschild-de Sitter space-time*, Gen. Rel. Grav. **31** 1703 (1999)

- [45] K. S. Virbhadra, & G. F. R. Ellis, *Schwarzschild black hole lensing*, Phys. Rev. **D62** 084003 (2000)